

## Coulomb repulsion and $T_c$ in BCS theory of superconductivity

X. H. Zheng\* and D. G. Walmsley

*Department of Pure and Applied Physics, The Queen's University of Belfast, Belfast BT7 1NN, Northern Ireland*

(Received 18 November 2004; published 19 April 2005)

Coulomb repulsion among the many electrons in a metal is in a balance, which can be toppled by even a weak electron-phonon attractive interaction. Therefore neglecting the Coulomb term from the BCS reduced Hamiltonian has little effect on  $T_c$ . This is shown by a field-theoretic argument, an analysis based on the Bogoliubov model potential and a direct numerical calculation. Detailed knowledge about electrons and phonons for various materials can be incorporated into the BCS theory through a refined treatment of the self-consistent gap equation. Consequently the universal ratio 3.5 in the BCS theory is replaced by a range of values varying from 3.51 for Ga to 4.76 for Hg. It is found that the phonon cutoff frequency is much lower than the Debye frequency. Extraordinarily high  $T_c$  could be expected if all phonons were involved in pairing electrons in a BCS superconductor.

DOI: 10.1103/PhysRevB.71.134512

PACS number(s): 74.20.Fg, 02.30.Rz

### I. INTRODUCTION

There have been varying views concerning the effect of Coulomb repulsion on superconductivity. According to Bardeen, Cooper, and Schrieffer (BCS) the criterion for superconductivity is that the attractive phonon interaction dominates the Coulomb interaction.<sup>1</sup> This view was tested numerically by Pines.<sup>2</sup> On the other hand, from the Bogoliubov model potential, it was found that Coulomb repulsion has little effect on  $T_c$ , the transition temperature of superconductors.<sup>3</sup> It is interesting that superconductivity may arise even with an entirely repulsive interaction, when this interaction is perturbed by an attractive interaction over a narrow range of phonon frequencies.<sup>3</sup> Which view should we follow?

There also have been varying views concerning the range of phonon frequencies involved in the electron-phonon interaction. BCS introduced the so-called average phonon frequency  $\omega$  which is also known as the cutoff frequency  $\omega_c$  because phonons stop pairing electrons when their frequencies exceed  $\omega_c$ .<sup>1</sup> However a liberty is often taken in the recent literature to let  $\omega_c$  equal  $\omega_D$ , the Debye frequency.<sup>3,4</sup> Should we follow this view?

There was no Coulomb term in the Hamiltonian in the original formalism of the canonical transform, which was introduced by Fröhlich and serves as the basis of the BCS theory.<sup>5</sup> In this transform the first order term of the electron-phonon interaction is cancelled. The second order term of this interaction perturbs the Bloch energy of the electrons to give  $2\Delta$ , the superconductive energy gap. We find that the formalism of the canonical transform is almost unchanged when we add the Coulomb term to the Hamiltonian. Now perturbed is not the Bloch energy but the energy of electrons with Coulomb repulsion. The energy gap itself remains almost the same. This reflects the fact that in a metal the Coulomb repulsion between electrons is in a balance, which may be toppled by even a weak electron-phonon interaction.

To test the above view of ours, we solve numerically the BCS self-consistent equation with and without Coulomb repulsion. The Coulomb interaction is screened with a variable screening radius. We find that superconductivity is almost

unaffected by the Coulomb repulsion. In particular in our calculation  $2\Delta/k_B T_c$  always stays exactly the same when the screening radius varies, where  $k_B$  is the Boltzmann constant. This explains why the BCS theory has been so successful without the Coulomb interaction.

In our calculation we use the electric conductivity of the metal to calibrate the strength of the electron-phonon interaction. We then vary the phonon cut-off frequency  $\omega_c$  until  $\Delta$  matches its experimental value. Our approach is justified because the calculated  $2\Delta/k_B T_c$ , which is beyond our control, also matches its experimental value. We find that on average the error in  $2\Delta/k_B T_c$  is less than 9% for 12 superconductive metals, including Hg and Pb. This enables us to predict  $T_c$  from the experimentally observed  $\Delta$ , or vice versa, fairly accurately.

We also find that the phonon cutoff frequency is much lower than the Debye frequency: on average  $\omega_c/\omega_D=0.15$  for the 12 superconductive metals. Apparently in BCS superconductors only a fraction of phonons is actually involved in pairing electrons, in accord with the view of a recent publication that superconductivity is frustrated when normal and umklapp scattering coexist.<sup>6</sup> If we were to let  $\omega_c=\omega_D$  then the transition temperature would become extraordinarily high, e.g.,  $T_c=980$  K for Sn. This appears to indicate room to raise  $T_c$  considerably if the frustration effect of umklapp scattering could somehow be eased.

### II. CANONICAL TRANSFORM WITHOUT COULOMB REPULSION

For the convenience of the reader we outline the major steps of the canonical transform by Fröhlich.<sup>5</sup> We start from the Hamiltonian without Coulomb repulsion

$$H = H_e + H_p + H_{e-p}. \quad (1)$$

Here  $H_e$  and  $H_p$  are electron and phonon Hamiltonians, respectively, and  $H_{e-p}$  the Hamiltonian of the electron-phonon interaction. We introduce the following general operator expansion (see the Appendix):

$$e^{-S}He^S = H + [H, S] + \frac{1}{2}[[H, S], S] + \dots, \quad (2)$$

$[H, S] = HS - SH$ . If we let

$$[H_e + H_p, S] + H_{e-p} = 0 \quad (3)$$

then by substituting Eqs. (1) and (3) into Eq. (2), and neglecting high order terms, we find

$$e^{-S}He^S = H_e + H_p + \frac{1}{2}[H_{e-p}, S], \quad (4)$$

where the first order term of the electron-phonon interaction is cancelled.

In order to evaluate Eq. (4) we appeal to second quantization, where the Hamiltonians are of the following form:

$$H_e = \sum_{\mathbf{k}, \sigma} \epsilon_{\mathbf{k}} a_{\mathbf{k}, \sigma}^{\dagger} a_{\mathbf{k}, \sigma}, \quad (5)$$

$$H_p = \sum_{\mathbf{q}, l} \hbar \omega_{\mathbf{q}, l} (c_{\mathbf{q}, l}^{\dagger} c_{\mathbf{q}, l} + 1/2), \quad (6)$$

$$H_{e-p} = -i \sum_{\mathbf{k}, \sigma, \mathbf{q}, l} \mathcal{M}_{\mathbf{q}, l} a_{\mathbf{k}+\mathbf{q}, \sigma}^{\dagger} a_{\mathbf{k}, \sigma} (c_{-\mathbf{q}, l}^{\dagger} + c_{\mathbf{q}, l}). \quad (7)$$

$a^{\dagger}$  and  $a$  are electron generation and destruction operators,  $\epsilon$  and  $\mathbf{k}$  electron energy and wave vector,  $\sigma$  spin,  $c^{\dagger}$  and  $c$  phonon generation and destruction operators, and  $\omega$  and  $\mathbf{q}$  phonon frequency and wave vector. Note that in Eq. (7) an electron has the same spin before and after being scattered by a phonon and  $l$  identifies phonon polarization. We neglect the slight dependence of the matrix element  $\mathcal{M}_{\mathbf{q}, l}$  on  $\mathbf{k}$ .<sup>1</sup> We are reminded that harmonic phonons are assumed in Eq. (7) in order to convert atomic displacement into  $c + c^{\dagger}$ .

According to Eq. (7) we have

$$\langle 0 | a_{\mathbf{k}+\mathbf{q}, \sigma} H_{e-p} a_{\mathbf{k}, \sigma}^{\dagger} c_{\mathbf{q}, l}^{\dagger} | 0 \rangle = -i \mathcal{M}_{\mathbf{q}, l}, \quad (8)$$

$$\langle 0 | a_{\mathbf{k}+\mathbf{q}, \sigma} c_{-\mathbf{q}, l} H_{e-p} a_{\mathbf{k}, \sigma}^{\dagger} | 0 \rangle = -i \mathcal{M}_{\mathbf{q}, l}, \quad (9)$$

$|0\rangle$  being the electron and phonon vacuum. Substituting Eq. (3) into Eqs. (8) and (9), we find through Eqs. (5) and (6) that

$$\langle 0 | a_{\mathbf{k}+\mathbf{q}, \sigma} S a_{\mathbf{k}, \sigma}^{\dagger} c_{\mathbf{q}, l}^{\dagger} | 0 \rangle = \frac{-i \mathcal{M}_{\mathbf{q}, l}}{\epsilon_{\mathbf{k}+\mathbf{q}} - \epsilon_{\mathbf{k}} - \hbar \omega_{\mathbf{q}, l}}, \quad (10)$$

$$\langle 0 | a_{\mathbf{k}+\mathbf{q}, \sigma} c_{-\mathbf{q}, l} S a_{\mathbf{k}, \sigma}^{\dagger} | 0 \rangle = \frac{-i \mathcal{M}_{\mathbf{q}, l}}{\epsilon_{\mathbf{k}+\mathbf{q}} - \epsilon_{\mathbf{k}} + \hbar \omega_{\mathbf{q}, l}}. \quad (11)$$

Equations (10) and (11) mean that we have

$$S = \sum_{\mathbf{k}, \sigma, \mathbf{q}, l} \frac{-i \mathcal{M}_{\mathbf{q}, l}}{\epsilon_{\mathbf{k}+\mathbf{q}} - \epsilon_{\mathbf{k}} - \hbar \omega_{\mathbf{q}, l}} a_{\mathbf{k}+\mathbf{q}, \sigma}^{\dagger} a_{\mathbf{k}, \sigma} c_{\mathbf{q}, l} + \sum_{\mathbf{k}, \sigma, \mathbf{q}, l} \frac{-i \mathcal{M}_{\mathbf{q}, l}}{\epsilon_{\mathbf{k}+\mathbf{q}} - \epsilon_{\mathbf{k}} + \hbar \omega_{\mathbf{q}, l}} a_{\mathbf{k}+\mathbf{q}, \sigma}^{\dagger} a_{\mathbf{k}, \sigma} c_{-\mathbf{q}, l}^{\dagger}, \quad (12)$$

which leads through Eq. (7) and the fermion and boson permutation relations to

$$[H_{e-p}, S] = - \sum_{\mathbf{k}, \mathbf{k}', \sigma, \sigma', \mathbf{q}} V_{\mathbf{k}, \mathbf{q}} a_{\mathbf{k}+\mathbf{q}, \sigma}^{\dagger} a_{\mathbf{k}', \sigma'}^{\dagger} a_{\mathbf{k}', \sigma'} a_{\mathbf{k}, \sigma} \quad (13)$$

with

$$V_{\mathbf{k}, \mathbf{q}} = \sum_l \frac{2 \hbar \omega_{\mathbf{q}, l} \mathcal{M}_{\mathbf{q}, l}^2}{(\hbar \omega_{\mathbf{q}, l})^2 - (\epsilon_{\mathbf{k}+\mathbf{q}} - \epsilon_{\mathbf{k}})^2}. \quad (14)$$

It is interesting that in Eq. (13) the phonon generation and destruction operators do not appear explicitly, i.e., we have virtual phonons which are emitted and then absorbed by the electrons but cannot be observed directly.

In the BCS theory the electrons are in pairs, with opposite momentum and spin, so that in Eq. (4) the operator  $e^{-S}He^S$  becomes

$$H_{\text{BCS}} = 2 \sum_{\mathbf{k}} \epsilon_{\mathbf{k}} b_{\mathbf{k}}^{\dagger} b_{\mathbf{k}} - \sum_{\mathbf{k}, \mathbf{q}} V_{\mathbf{k}, \mathbf{q}} b_{\mathbf{k}+\mathbf{q}}^{\dagger} b_{\mathbf{k}} \quad (15)$$

which is known as the BCS reduced Hamiltonian, where

$$b_{\mathbf{k}} = a_{-\mathbf{k}, \downarrow} a_{\mathbf{k}, \uparrow}, \quad b_{\mathbf{k}}^{\dagger} = a_{\mathbf{k}, \uparrow}^{\dagger} a_{-\mathbf{k}, \downarrow}^{\dagger} \quad (16)$$

are pair generation and destruction operators,  $\uparrow$  and  $\downarrow$  spins. In Eq. (15) the electron term is also in  $b$ , which vanishes when applied to single electrons. When  $T > 0$ , we have to replace the first summation in Eq. (15) with the standard electron Hamiltonian in Eq. (5) in order to take into account the energy of single electrons.<sup>1</sup> It is no longer necessary to have the phonon Hamiltonian  $H_p$  explicitly involved in Eq. (15) when phonons become virtual.

### III. CANONICAL TRANSFORM WITH COULOMB REPULSION

Now we replace Eq. (1) with

$$H = H_e + H_p + H_{e-p} + H_{\text{Col}}, \quad (17)$$

where  $H_{\text{Col}}$  is the Hamiltonian of Coulomb repulsion. We also replace Eq. (3) with

$$[H_e + H_p + H_{\text{Col}}, S] + H_{e-p} = 0. \quad (18)$$

Consequently Eq. (4) becomes

$$e^{-S}He^S = H_e + H_{\text{Col}} + H_p + \frac{1}{2}[H_{e-p}, S] \quad (19)$$

and Eq. (15) becomes

$$H_{\text{BCS}} + H_{\text{Col}} = 2 \sum_{\mathbf{k}} \epsilon_{\mathbf{k}} b_{\mathbf{k}}^{\dagger} b_{\mathbf{k}} - \sum_{\mathbf{k}, \mathbf{q}} (V_{\mathbf{k}, \mathbf{q}} - U_{\mathbf{q}}) b_{\mathbf{k}+\mathbf{q}}^{\dagger} b_{\mathbf{k}} \quad (20)$$

with<sup>2</sup>

$$U_{\mathbf{q}} = \frac{e^2}{4\pi\epsilon_0} \frac{\Omega^{-1}}{q^2 + q_0^2}. \quad (21)$$

Here  $q_0$  measures the screening radius,  $e$  is the electron charge, and  $\epsilon_0$  vacuum permittivity. We have adopted the SI unit system where the Coulomb interaction is  $e^2/4\pi\epsilon_0 r$  between two electrons at distance  $r$ . Equation (21) arises from a Fourier integration over  $\mathbf{q}$  which is continuous. We convert

this integration into the summation in Eq. (20) over discrete  $\mathbf{q}$  and this leads to the factor  $\Omega^{-1}$  in Eq. (21), which is the inverse of the total volume of the metal, to replace  $d\mathbf{q}$  in the integration.

Equation (20) appears to suggest  $V_{\mathbf{k},\mathbf{q}} > U_{\mathbf{k}}$  as the criterion for superconductivity. However, if we replace Eq. (1) with Eq. (17), and replace Eq. (5) with

$$H_e + H_{\text{Col}} = \sum_{\mathbf{k}} \tilde{\epsilon}_{\mathbf{k}} a_{\mathbf{k}}^+ a_{\mathbf{k}}, \quad (22)$$

$\tilde{\epsilon}_{\mathbf{k}}$  being the electron energy *with* Coulomb repulsion, then we find through the canonical transform in the previous section

$$\tilde{H}_{\text{BCS}} = 2 \sum_{\mathbf{k}} \tilde{\epsilon}_{\mathbf{k}} b_{\mathbf{k}}^+ b_{\mathbf{k}} - \sum_{\mathbf{k},\mathbf{q}} \tilde{V}_{\mathbf{k},\mathbf{q}} b_{\mathbf{k}+\mathbf{q}}^+ b_{\mathbf{k}} \quad (23)$$

which is almost identical to Eq. (15), with

$$\tilde{V}_{\mathbf{k},\mathbf{q}} = \sum_l \frac{2\hbar\omega_{\mathbf{q},l} \mathcal{M}_{\mathbf{q},l}^2}{(\hbar\omega_{\mathbf{q},l})^2 - (\tilde{\epsilon}_{\mathbf{k}+\mathbf{q}} - \tilde{\epsilon}_{\mathbf{k}})^2} \quad (24)$$

which too is almost identical to Eq. (14).

In the above argument Eq. (22) is introduced as a reasonable assumption, namely,  $H_e + H_{\text{Col}}$  has eigenfunctions, which are orthogonal to each other with  $\tilde{\epsilon}_{\mathbf{k}}$  as their eigenvalue. There could be some technical difficulty if we try to calculate  $\tilde{\epsilon}_{\mathbf{k}}$  from first principles. However, we are mainly interested in how much  $\tilde{\epsilon}_{\mathbf{k}}$  is perturbed by  $\tilde{V}_{\mathbf{k},\mathbf{q}}$  rather than the actual values of  $\tilde{\epsilon}_{\mathbf{k}}$ . It is apparent from Eq. (24) that, when we evaluate  $\tilde{V}_{\mathbf{k},\mathbf{q}}$ , we have to evaluate both  $\tilde{\epsilon}_{\mathbf{k}}$  and  $\tilde{\epsilon}_{\mathbf{k}+\mathbf{q}}$  at the same time. It is not an issue that  $\tilde{\epsilon}_{\mathbf{k}}$  may differ from the Bloch energy  $\epsilon_{\mathbf{k}}$  by an infinity, since it will be cancelled in Eq. (24). The issue here is that the dispersion relation, which relates the electron energy and momentum, could be slightly distorted in the presence of the Coulomb repulsion, so that  $\epsilon_{\mathbf{k}+\mathbf{q}} - \epsilon_{\mathbf{k}}$  in Eq. (14) may differ slightly from  $\tilde{\epsilon}_{\mathbf{k}+\mathbf{q}} - \tilde{\epsilon}_{\mathbf{k}}$  in Eq. (24) for the same value of  $\mathbf{q}$ . In this respect Coulomb repulsion may have little effect on superconductivity.

The unimportance of Coulomb repulsion, with respect to its effect on superconductivity, could be explained as follows: attraction due to electron-phonon interaction, though weak, is sufficient to topple the balance of the Coulomb force among the many electrons in a metal. As a result  $\tilde{V}$  and  $V$  are almost identical in Eqs. (24) and (14), which are derived with and without the Coulomb Hamiltonian, respectively.

#### IV. BOGOLIUBOV MODEL POTENTIAL

Equation (20) leads to the self-consistent gap equation

$$\Delta(\mathbf{k}) = \sum_{\mathbf{q}} (V_{\mathbf{k},\mathbf{q}} - U_{\mathbf{k}}) \frac{\Delta(\mathbf{k} + \mathbf{q})}{2E(\mathbf{k} + \mathbf{q})}, \quad (25)$$

where  $\Delta$  measures the superconductive energy gap,  $E = (\Delta^2 + \epsilon^2)^{1/2}$ . Equation (25) can also be written as

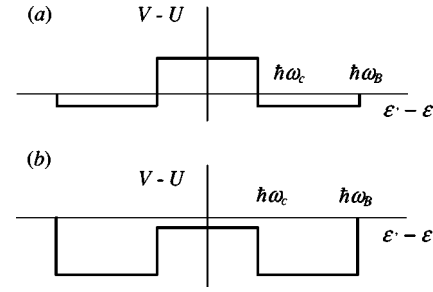


FIG. 1. Bogoliubov model potential, where  $U_{\mathbf{q}}$  and  $V_{\mathbf{k},\mathbf{q}}$  are modeled by  $U$  and  $V$ , which distribute uniformly when  $|\epsilon' - \epsilon| < \omega_B$  and  $\omega_c$ , respectively. (a)  $V$  dominates when  $|\epsilon' - \epsilon| < \omega_c$ . (b)  $U$  always dominates.

$$\Delta(\epsilon) = N(0) \int V(\epsilon' - \epsilon) \frac{\Delta(\epsilon')}{2E(\epsilon')} d\epsilon' - N(0) \int U(\epsilon' - \epsilon) \frac{\Delta(\epsilon')}{2E(\epsilon')} d\epsilon'. \quad (26)$$

$\epsilon$  represents energy relative to the Fermi surface and  $N(0)$  the density of states.<sup>1</sup>

In order to solve Eq. (26) analytically, Bogoliubov devised a model potential, where

$$V(\epsilon' - \epsilon) = \begin{cases} V, & |\epsilon' - \epsilon| < \hbar\omega_c, \\ 0, & \text{otherwise,} \end{cases} \quad (27)$$

whereas

$$U(\epsilon' - \epsilon) = \begin{cases} U, & |\epsilon' - \epsilon| < \hbar\omega_B, \\ 0, & \text{otherwise,} \end{cases} \quad (28)$$

$\omega_B$  is known as the Coulomb cutoff frequency (see Fig. 1).<sup>3</sup> It is also assumed that  $\Delta(\epsilon)$  takes only two values. Furthermore, it is assumed that, when  $\Delta(\epsilon) = \Delta_1$ , values of  $\epsilon$  and  $\epsilon'$  are such that  $V(\epsilon' - \epsilon) = V$  and  $U(\epsilon' - \epsilon) = U$ . On the other hand, when  $\Delta(\epsilon) = \Delta_2$ , we are supposed to have  $V(\epsilon' - \epsilon) = 0$  and  $U(\epsilon' - \epsilon) = U$ .<sup>3</sup> As a result, we find from Eq. (26) a pair of algebraic equations

$$\begin{bmatrix} \Delta_1 \\ \Delta_2 \end{bmatrix} = \begin{bmatrix} (\lambda - \mu)I_1 & -\mu I_2 \\ -\mu I_1 & -\mu I_2 \end{bmatrix} \begin{bmatrix} \Delta_1 \\ \Delta_2 \end{bmatrix}, \quad (29)$$

where  $\lambda = N(0)V$ ,  $\mu = N(0)U$ ,

$$I_1 = \int_0^{\hbar\omega_c} \frac{d\epsilon'}{(\epsilon'^2 + \Delta_1^2)^{1/2}} = \sinh^{-1} \left( \frac{\hbar\omega_c}{\Delta_1} \right), \quad (30)$$

$$I_2 = \int_{\hbar\omega_c}^{\hbar\omega_B} \frac{d\epsilon'}{(\epsilon'^2 + \Delta_2^2)^{1/2}} \approx \ln \left( \frac{\omega_B}{\omega_c} \right). \quad (31)$$

Equation (30) is exact. Equation (31) tells us that  $I_2$  becomes larger the larger the ratio  $\omega_B/\omega_c$ .

Equation (29) has a nontrivial solution only when

$$\begin{vmatrix} 1 - (\lambda - \mu)I_1 & \mu I_2 \\ \mu I_1 & 1 + \mu I_2 \end{vmatrix} = 0 \quad (32)$$

which means

$$I_1 = \left( \lambda - \frac{\mu}{1 + \mu I_2} \right)^{-1}. \quad (33)$$

When  $\omega_B \gg \omega_c$ , Eq. (33) is reduced to  $I_1 = \lambda^{-1}$ , or

$$\Delta_1 = \hbar \omega_c / \sinh[1/N(0)V] \quad (34)$$

which is exactly the expression for the energy gap function in the BCS theory without Coulomb repulsion. Apparently the value of  $U$  has little effect on  $\Delta_1$  when the Coulomb cutoff frequency of Bogoliubov  $\omega_B$  is large enough. It is interesting that  $\Delta_1$  may arise even with the entirely repulsive potential in Fig. 1(b).

In Ref. 3 the Bogoliubov model potential is used to discuss the effect of Coulomb repulsion on  $T_c$ . The discussion is essentially based on the relation  $2\Delta_1/k_B T_c = 3.5$ , with the apparent consequence that the Coulomb repulsion has little effect on  $T_c$ . On the other hand, the ratio  $\omega_B/\omega_c$  is shown not to have significant effect on the isotope coefficient.<sup>3</sup>

## V. MATRIX ELEMENT AND ADIABATIC PARAMETER

Now we evaluate  $V_{\mathbf{k},\mathbf{q}}$  in Eq. (14), in order to solve the self-consistent gap equation (25) numerically. The expression for the matrix element

$$\mathcal{M}_{\mathbf{q},l} = \tilde{q}_l \left( \frac{N\hbar}{2M\omega_{ql}} \right)^{1/2} \int_{\Omega_0} \psi_{\mathbf{k}+\mathbf{q},\sigma}^*(\mathbf{r}) [\mathcal{V}(\mathbf{r}) - \mathcal{V}(0)] \psi_{\mathbf{k},\sigma}(\mathbf{r}) d\mathbf{r} \quad (35)$$

is well known.<sup>7,8</sup> Here  $\mathcal{V}$  is the atomic potential,  $\psi$ 's electron wave functions (Bloch functions),  $M$  atomic mass,  $N$  number of atoms in unit volume,  $\sum_l \tilde{q}_l^2 = q^2$ ,  $\mathbf{r}$  coordinates in real space, and  $\Omega_0$  the Wigner-Seitz cell. When  $\mathcal{V}$  is symmetric with respect to the atomic site, Eq. (35) can be evaluated analytically to give<sup>7,8</sup>

$$\sum_l 2\hbar\omega_{ql} |\mathcal{M}_{\mathbf{q},l}|^2 = \frac{\hbar^2 q^2 (\delta\mathcal{V})^2}{NM} F^2(\tau). \quad (36)$$

$F(\tau) = 3(\sin \tau - \tau \cos \tau) / \tau^3$ ,  $\tau = r_0 q$ ,  $r_0$  radius of  $\Omega_0$  (assumed to be spherical), and  $\delta\mathcal{V} = \mathcal{V}(r_0) - \mathcal{V}(0)$  atomic potential measured from the atom site. Letting

$$\xi = q/2k_F, \quad (37)$$

$k_F$  being the Fermi momentum, for a spherical Fermi surface we have  $k_F = (3\pi^2 Z / \Omega_0)^{1/3}$ ,  $\Omega_0 = (4\pi/3)r_0^3$ ,  $Z$  the valency, so that  $\tau = 2k_F r_0 \xi = (18\pi Z)^{1/3} \xi = 3.84Z^{1/3} \xi$ .

We parametrize the electron energy in the usual way:<sup>9</sup>

$$\epsilon_{\mathbf{k}} = \sqrt{(v_F p_1)^2 + (v_2 p_2)^2}, \quad (38)$$

where the momentum  $\mathbf{p}$  is measured from the Fermi surface, with  $p_1$  and  $p_2$  normal and parallel to it,  $v_F$  is the Fermi velocity. We may understand that  $p_1$ ,  $p_2$ , and  $v_F$  are found with or without Coulomb repulsion. In the former case we should replace  $\epsilon_{\mathbf{k}}$  with  $\tilde{\epsilon}_{\mathbf{k}}$ . Equation (38) applies above the Fermi surface, but can be easily extended to  $\epsilon_{\mathbf{k}}$  below it.<sup>10,11</sup> For a spherical Fermi surface  $p_1 = \hbar(k - k_F)$  and  $p_2 = 0$ ,  $k_F$  being the Fermi wave number, so that

TABLE I. Calculated physical properties and corresponding experimental values for a range of superconducting elements.

	$\Delta_0^{a,b}$	$U_0^b$	$\delta^c$	$\omega_c/\omega_D$	$2\Delta(0)/k_B T_c^d$
Zn	1.19 (1.20)	6840	1.50	0.167	3.63 (3.20)
Cd	0.26 (0.75)	5040	1.20	0.245	3.70 (3.20)
Hg	0.81 (8.25)	4900	0.44	0.124	4.76 (4.60)
Al	1.37 (1.70)	6300	1.81	0.183	3.54 (3.30)
Ga	3.96 (1.65)	5960	1.51	0.096	3.51 (3.50)
In	0.25 (5.25)	5420	0.62	0.203	3.92 (3.60)
Tl	0.23 (3.68)	5260	0.48	0.164	3.92 (3.57)
Sn	1.26 (5.75)	5440	1.25	0.158	3.70 (3.50)
Pb	0.70 (13.7)	5670	0.60	0.160	4.56 (4.38)
V	14.0 (8.00)	7930	1.20	0.068	3.95 (3.40)
Nb	4.90 (15.3)	7270	1.04	0.107	4.25 (3.80)
Ta	3.36 (7.00)	8110	0.90	0.095	3.95 (3.60)

<sup>a</sup>Values of  $\Delta(0)$  bracketed.

<sup>b</sup>In  $10^{-4}$  eV.

<sup>c</sup>In  $10^{-3}$ .

<sup>d</sup>Experimental data bracketed.

$$\epsilon_{\mathbf{k}+\mathbf{q}} - \epsilon_{\mathbf{k}} = \hbar v_F q x \quad (39)$$

near the Fermi surface,  $x = \xi + \cos \theta$ ,  $\theta$  being the angle between  $\mathbf{k}$  and  $\mathbf{q}$ . In the Debye phonon model  $\omega_{ql} = v_D q$ ,  $v_D$  being the sound velocity, giving

$$(\hbar\omega_{ql})^2 - (\epsilon_{\mathbf{k}+\mathbf{q}} - \epsilon_{\mathbf{k}})^2 = \hbar^2 v_F^2 q^2 (\delta^2 - x^2), \quad (40)$$

where

$$\delta = \frac{v_D}{v_F} = \frac{k_F}{2q_D} \frac{\hbar\omega_D}{\epsilon_F} = \left( \frac{\pi}{16} \right)^{1/3} \frac{T_D}{T_F}. \quad (41)$$

$q_D$  is the Debye wave number,  $\epsilon_F = (\hbar/2)v_F k_F$ ,  $T_D$  and  $T_F$  Debye and Fermi temperatures. We see from Table I that  $\delta \sim 10^{-3}$ , which is known as the adiabatic parameter in the literature.<sup>12</sup> In more realistic models the sound velocity may depend on  $\mathbf{q}$  so that  $\delta$  may not be constant. By substituting Eqs. (36) and (40) into Eq. (24), we find

$$V_{\mathbf{k},\mathbf{q}} = \frac{(\delta\mathcal{V})^2 F^2(3.84Z^{1/3}\xi)}{NMv_F^2 (\delta^2 - x^2)}. \quad (42)$$

$\delta\mathcal{V}$  and  $\delta$  are defined in Eqs. (36) and (41), respectively.

## VI. ATOMIC POTENTIAL

In order to evaluate Eq. (42) we have to know  $\delta\mathcal{V}$ . Carbotte and Dynes utilized tabulated data of the Heine-Abarenkov pseudopotential to estimate  $\delta\mathcal{V}$  and calculated the electric resistivity  $\rho$  and energy gap  $\Delta$  (using the Eliashberg formalism) separately.<sup>13,14</sup> However, we do not have to calculate  $\delta\mathcal{V}$  explicitly. According to Mott and Jones<sup>8</sup> the resistivity of a metal is given by the following formula:



$$\rho = \frac{12\pi(\delta V)^2}{NMv_F^2} \frac{k_B T_\rho}{\hbar e^2 v_D^2} I. \quad (43)$$

$k_B$  is the Boltzmann constant,  $T_\rho$  the temperature (room temperature) when  $\rho$  is measured,  $e$  electronic charge, and

$$I = \int_0^{\xi_D} F^2(3.84Z^{1/3}\xi) \xi^3 d\xi, \quad (44)$$

where

$$\xi_D = q_D/2k_F = 1/(4Z)^{1/3}, \quad (45)$$

$q_D$  being the Debye cutoff momentum. Combining Eqs. (42) and (43), we find

$$V_{\mathbf{k},\mathbf{q}} = \frac{1}{12\pi I} \frac{\hbar e^2 \rho v_D^2}{k_B T_\rho} \frac{F^2(3.84Z^{1/3}\xi)}{\delta^2 - x^2} \quad (46)$$

which can be readily evaluated.

### VII. SELF-CONSISTENT GAP EQUATION WITHOUT COULOMB REPULSION

We drop  $U_{\mathbf{q}}$  from Eq. (25) and integrate the resultant equation in a phonon sphere of radius  $q$ . We use Eq. (46) to evaluate  $V_{\mathbf{k},\mathbf{q}}$ . After some algebra, we find

$$\begin{aligned} \Delta(\epsilon) &= \frac{\Delta_0}{2\pi I} \int_0^{\xi_c} F^2(3.84Z^{1/3}\xi) \xi^2 d\xi \\ &\times \int_{\xi-1}^{\xi+1} \frac{\Delta(\epsilon + 4\epsilon_F \xi x)}{E(\epsilon + 4\epsilon_F \xi x)} \frac{dx}{\delta^2 - x^2}, \end{aligned} \quad (47)$$

where  $I$  is defined in Eq. (44),

$$\Delta_0 = \hbar e^2 n \rho v_D^2 / 2k_B T_\rho, \quad (48)$$

$n=ZN$  being the number of electrons in unit volume.

We see from Table I that the value of  $\Delta_0$  is often close to measured values of  $\Delta$ . In order to understand the physical reason of this, we integrate  $V_{\mathbf{k},\mathbf{q}}$  in Eq. (46) over the first phonon Brillouin zone, and find

$$\sum_{\mathbf{q}} V_{\mathbf{k},\mathbf{q}} = \frac{\Delta_0}{2\pi I} \int_0^{\xi_D} F^2(3.84Z^{1/3}\xi) \xi^2 d\xi \int_{\xi-1}^{\xi+1} \frac{dx}{\delta^2 - x^2} \quad (49)$$

which can be compared with Eq. (47). We have

$$\int_{\xi-1}^{\xi+1} \frac{dx}{\delta^2 - x^2} = \frac{2}{1 - \xi^2} \quad (50)$$

when  $\delta \ll 1$ . We also have

$$\int_0^{\xi_D} F^2(3.84Z^{1/3}\xi) \frac{\xi^2 d\xi}{1 - \xi^2} \approx \pi I, \quad (51)$$

where  $I$  is given by Eq. (44). Combining Eqs. (49)–(51) we find

$$\sum_{\mathbf{q}} V_{\mathbf{k},\mathbf{q}} \approx \Delta_0 \quad (52)$$

which tells us that  $\Delta_0$  is a parameter to measure the strength of electron-phonon interaction. It is apparent from Eq. (48)

that strong electron-phonon interaction arises from numerous free electrons (large  $n$ ) scattered frequently by atoms (large  $\rho$ ) that move quickly (large  $v_D$ ) to facilitate pairing.

### VIII. ITERATION ALGORITHM

We solve Eq. (47) through iteration. In each of the iterations we have to vary  $\xi_c$  in order to let  $\Delta(0)$  match its experimental value. This means that we have to integrate Eq. (47) many times with varying  $\xi_c$ . The resultant  $\Delta(\epsilon)$ , with correct  $\Delta(0)$ , is substituted into the right-hand side of Eq. (47) for the next round of iteration. This process is repeated until iteration makes little difference in  $\Delta(\epsilon)$  [on average  $<\Delta(0) \times 10^{-7}$ ].

It is actually quite laborious to integrate Eq. (47), not only because the integration is 2D, but also because the second integration in Eq. (47) exists in the sense of the Cauchy principal value,<sup>15</sup> whose numerical evaluation is particularly demanding around the two poles of  $1/(x^2 - \delta^2)$ . We evaluate the Cauchy principal value semianalytically. The integrand  $\Delta/E$  is assumed to be linear in small intervals of  $x$ , and is integrated analytically. This saves us enormous computer time.

In order to check our numerical result, we notice that in first iteration, when we set  $\Delta = \Delta_0$ , the Cauchy principal value in Eq. (47) has an analytical form

$$\begin{aligned} &\int \frac{\Delta_0}{\sqrt{\Delta_0^2 + (\epsilon + 4\epsilon_F \xi x)^2} \delta^2 - x^2} dx \\ &= \frac{\Delta_0/2\delta}{\sqrt{\Delta_0^2 + (\epsilon + 4\epsilon_F \xi \delta)^2}} \ln \frac{2A(x)}{|x - \delta|} \\ &\quad - \frac{\Delta_0/2\delta}{\sqrt{\Delta_0^2 + (\epsilon - 4\epsilon_F \xi \delta)^2}} \ln \frac{2B(x)}{|x + \delta|} + C, \end{aligned} \quad (53)$$

where  $C$  is the integration constant

$$\begin{aligned} A(x) &= \Delta_0^2 + (\epsilon + 4\epsilon_F \xi \delta)(\epsilon + 4\epsilon_F \xi x) \\ &\quad + \sqrt{\Delta_0^2 + (\epsilon + 4\epsilon_F \xi \delta)^2} \sqrt{\Delta_0^2 + (\epsilon + 4\epsilon_F \xi x)^2}, \end{aligned}$$

$$\begin{aligned} B(x) &= \Delta_0^2 + (\epsilon - 4\epsilon_F \xi \delta)(\epsilon + 4\epsilon_F \xi x) \\ &\quad + \sqrt{\Delta_0^2 + (\epsilon - 4\epsilon_F \xi \delta)^2} \sqrt{\Delta_0^2 + (\epsilon + 4\epsilon_F \xi x)^2}. \end{aligned}$$

The solution based on Eq. (53) is virtually identical to the full numerical solution of Eq. (47) in first iteration. It can be seen from Fig. 2 that prominent features of  $\Delta(\epsilon)$  have already emerged from first iteration: further iterations improve the accuracy of solution but retain the physics.

### IX. GAP FUNCTION WITHOUT COULOMB REPULSION

One prominent feature of  $\Delta(\epsilon)$  lies in its structure: it has a peak flanked by two negative dips. For tin the distance between the peak and one dip is  $\sim 4$  meV (Fig. 2) compared with  $\hbar\omega_D = 17$  meV. As a result, the curve of  $d\epsilon/dE$ , which represents the tunneling density of states, also has a structure featuring a dip, similar to the characteristic dip in the tunneling experiment data.<sup>16</sup> Indeed  $\Delta(\epsilon)$  is also structured in the numerical solutions for the Eliashberg equation.<sup>16–18</sup>

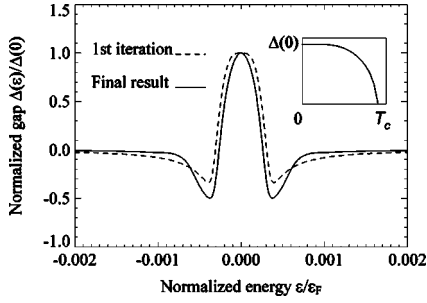


FIG. 2.  $\Delta(\epsilon)$  curve for Sn at  $T=0$ . The temperature curve of  $\Delta(0)$  is shown in the inset.

Another prominent feature is that  $\omega_c/\omega_D \ll 1$  (0.148 on average for the 12 metals in Table I). This is somewhat puzzling because, assuming that  $\Delta/E$  varies slowly over the range of phonon frequencies, we can integrate Eq. (25) (without  $U_q$ ) over the first Brillouin zone and find  $\Delta(0) \approx \Delta_0/2$  (true in many cases in Table I). Specifically, if we let

$$\frac{\Delta(\mathbf{k} + \mathbf{q})}{E(\mathbf{k} + \mathbf{q})} = \frac{\Delta(\mathbf{k})}{E(\mathbf{k})} \quad (54)$$

then Eq. (25) becomes  $E(\mathbf{k}) = (1/2) \sum_{\mathbf{q}} V_{\mathbf{k},\mathbf{q}}$ , which leads through Eq. (52) to

$$\Delta(0) = (1/2) \sum_{\mathbf{q}} V_{\mathbf{k},\mathbf{q}} \approx \Delta_0/2, \quad (55)$$

where  $\mathbf{q}$  runs over the first phonon Brillouin zone: Eq. (45) is assumed (i.e.,  $\omega_c/\omega_D$  not small). However  $\Delta/E$  is by no means slowly varying but has the shape of a sharp peak, as is shown in Fig. 3, in contrast to the assumption in Eq. (54). It is also clear from Fig. 3 that, when  $\epsilon=0$ , the peak of  $\Delta/E$  samples the extremely large and positive values of  $V_{\mathbf{k},\mathbf{q}}$  [proportional to  $1/(\delta^2 - x^2)$ , see Eqs. (24) and (40)] that would have been cancelled by the equally large but negative values

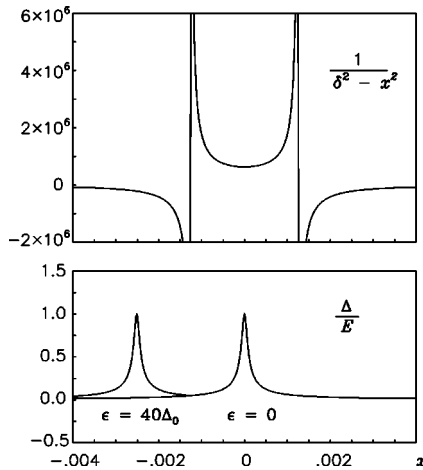


FIG. 3. Factors of the integrand in Eq. (25) or (47) in first iteration (when  $\Delta = \Delta_0$ ),  $\Delta_0$  and  $\delta$  are evaluated for Sn (Table I), with  $\xi = q/2k_F = 0.05$ . Upper: values of  $1/(\delta^2 - x^2)$  (proportional to  $V_{\mathbf{k},\mathbf{q}}$ ). Lower: values of  $\Delta_0/E$ , with the shape of a peak, whose position shifts when  $\epsilon$  varies. Apparently the position of this peak determines the sign and value of the integrand.

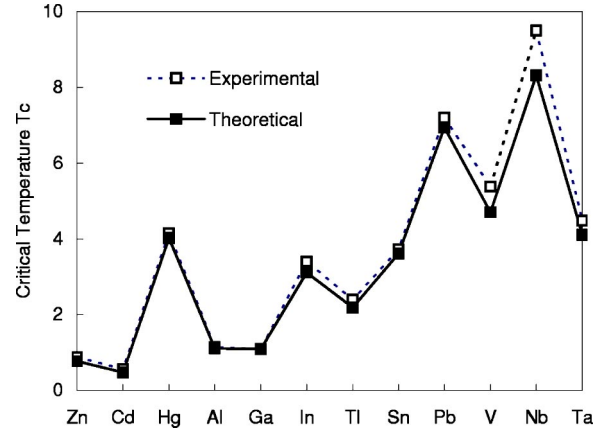


FIG. 4. Experimental and theoretical values of  $T_c$  found from  $\Delta(0)$ ,  $\Delta_0$ , and  $\delta$  in Table I. On average the difference between theory and experiment  $< 0.3$  K.

of  $V_{\mathbf{k},\mathbf{q}}$  at  $x < \Delta$ , had  $\Delta/E$  been slowly varying. As a result  $\Delta(0)$  will vastly exceed its experimental value unless  $\omega_c/\omega_D \ll 1$ . On the other hand, when  $\epsilon > 0$ , the peak of  $\Delta/E$  may sample the negative values of  $V_{\mathbf{k},\mathbf{q}}$ , and this leads to the dips and extended negative wings of  $\Delta(\epsilon)$  in Fig. 2.

### X. $T_c$ WITHOUT COULOMB REPULSION

In order to justify the values of  $\omega_c/\omega_D$  in Table I we solve the following self-consistent equation

$$\begin{aligned} \Delta(\epsilon, T) = & \frac{\Delta_0}{2\pi I} \int_0^{\xi_c} F^2(3.84Z^{1/3}\xi) \xi^2 d\xi \\ & \times \int_{\xi-1}^{\xi+1} \tanh \frac{E(\epsilon + 4\epsilon_F \xi x, T)}{2k_B T} \\ & \times \frac{\Delta(\epsilon + 4\epsilon_F \xi x, T)}{E(\epsilon + 4\epsilon_F \xi x, T)} \frac{dx}{\delta^2 - x^2} \end{aligned} \quad (56)$$

for  $T > 0$ , which is identical to Eq. (47), save an additional factor  $\tanh(E/2k_B T)$  in the integrand.<sup>1</sup> Now  $\Delta$  and  $E$  are marked as  $\Delta(\epsilon, T)$  and  $E(\epsilon, T)$  [ $\Delta(\epsilon)$  and  $E(\epsilon)$  imply  $T=0$ ].

We also solve Eq. (56) through iteration. We find  $\xi_c$  at  $T=0$  (see Sec. VIII) and it is kept unchanged thereafter.<sup>1</sup> We let  $T$  increase in small steps and use converged  $\Delta(\epsilon, T)$  to start iteration at the next  $T$ . We find  $T_c$  through a quadratic curve fit once  $\Delta(0, T) < 0.01\Delta(0)$ . We find reasonably accurate  $T_c$  (average error  $< 0.3$  K, Fig. 4) and  $2\Delta(0)/k_B T_c$  (average error 8.9%, Table I). In particular the large measured values 4.6 and 4.38 for Hg and Pb have been calculated fairly successfully given the simplicity of the model.

The ratio  $2\Delta(0)/k_B T_c = 3.5$  is one of the great triumphs of the BCS theory. On the other side of the coin, one could be lured to believe that the BCS theory is incapable of producing other ratios for elements such as Hg and Pb unless some new physics is introduced. Now we see that the BCS theory is capable of producing other ratios provided that a refined treatment is introduced. In this treatment we do not average  $V_{\mathbf{k},\mathbf{q}}$  over the phonon spectrum. We also adjust the adiabatic

TABLE II. Effect of Coulomb screening on  $T_c$  and  $\omega_c$ .

$\xi_0^a$	$\omega_c/\omega_D$	$T_c^b$	$\xi_0^a$	$\omega_c/\omega_D$	$T_c^b$
0.1	0.168	3.64	0.6	0.160	3.64
0.2	0.164	3.64	0.7	0.159	3.64
0.3	0.162	3.64	0.8	0.159	3.64
0.4	0.161	3.64	0.9	0.159	3.64
0.5	0.160	3.64	$\infty$	0.158	3.64

<sup>a</sup> $\xi_B = \xi_D$ .

<sup>b</sup>For Sn (experimental value=3.72, in K).

parameter,  $\delta$ , and cutoff frequency  $\omega_c$  in accordance with the experimental data of the elements. Therefore we are allowed to incorporate more comprehensive knowledge about the electrons and phonons into the BCS theory. Indeed  $\delta$  is the ratio between the Debye and Fermi velocities, see Eq. (41), of which the latter is all we need to know about the electrons when we assume a Fermi sea. On the other hand, the Debye velocity is all we need to know about Debye phonons. We follow BCS to cut the phonon frequency off at  $\omega_c$  to take into account the hitherto unnoticed frustration effect of umklapp scattering.<sup>6</sup> In a more realistic phonon model we may not have the simple relation  $\omega_{q,l} = v_{Dl}q$  so that, according to Eqs. (40) and (41),  $\delta$  may not be a constant. This could be used to introduce further refined treatment to the BCS theory.

### XI. $T_c$ WITH COULOMB REPULSION

When the Coulomb repulsion is included, we use Eq. (20) to derive the self-consistent equation which, at  $T=0$ , is identical to Eq. (47) apart from the following additional term

$$U_0 \int_0^{\xi_B} \frac{\xi^2}{\xi^2 + \xi_0^2} d\xi \int_{\xi-1}^{\xi+1} \frac{\Delta(\epsilon + 4\epsilon_F \xi x)}{E(\epsilon + 4\epsilon_F \xi x)} dx \quad (57)$$

on its right-hand side, where

$$U_0 = \frac{e^2}{4\pi\epsilon_0} \frac{k_F}{(2\pi)^2} \quad (58)$$

whose values can be found in Table I. When  $T > 0$  we add Eq. (57), with an additional factor  $\tanh(E/2k_B T)$  in the integrand, to the right-hand side of Eq. (56).

We solve the self-consistent equation, with Coulomb repulsion, for tin. We again use the iteration method, where the

 TABLE III. Effect of Bogoliubov cutoff frequency in Coulomb interaction on  $T_c$  and  $\omega_c$ .

$\xi_B^a$	$\omega_c/\omega_D$	$T_c^b$	$\xi_B^a$	$\omega_c/\omega_D$	$T_c^b$
1	0.160	3.64	6	0.164	3.64
2	0.163	3.64	7	0.164	3.64
3	0.164	3.64	8	0.164	3.64
4	0.164	3.64	9	0.164	3.64
5	0.164	3.64	10	0.164	3.64

<sup>a</sup>In  $\xi_D$  ( $\xi_0=0.5$ ).

<sup>b</sup>For Sn (experimental value=3.72, in K).

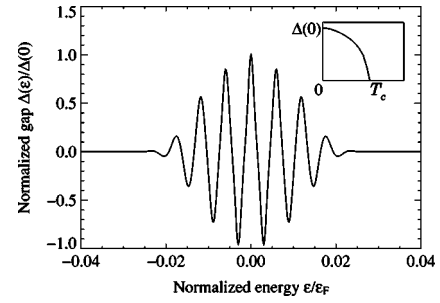


FIG. 5.  $\Delta(\epsilon)$  of Sn without umklapp scattering. The temperature curve of  $\Delta(0)$  is in the inset.

value of  $\xi_c$  is again varied to let  $\Delta(0)$  match the experimental data, as we did in Sec. VIII. We vary  $\xi_0$  in expression (57) to test the effect of screening. The iteration solution converges well when  $\xi_0 \geq 0.1$ . We see from Table II that  $\xi_0$  has no effect on  $T_c$ . In expression (57) the value of  $\xi_B$  is always fixed at between  $\xi_D$  and  $10\xi_D$ , which is large compared with  $\xi_c$ , for the reason that there is no upper limit for the phonon frequency in the Coulomb interaction. We see from Table III that  $\xi_B$  also has no effect on  $T_c$ .

### XII. DEBYE CUTOFF FREQUENCY

In the recent literature a liberty is often taken to replace the phonon cutoff frequency  $\omega_c$  in Eq. (27) with the Debye cutoff frequency  $\omega_D$ . That amounts to replacing  $\xi_c$  in Eq. (47) with  $\xi_D$  in Eq. (45). In Eq. (47) the integration with respect to  $\xi$  is roughly proportional to  $\xi_c^3$ , which in turn is proportional to  $\omega_c^3$ . If we replace  $\omega_c$  with  $\omega_D$  then the gap function will be enlarged by a factor  $(\omega_D/\omega_c)^3$ . Consequently we will have

$$T_c \approx (\omega_D/\omega_c)^3 T_c^{\text{exp}}, \quad (59)$$

$T_c^{\text{exp}}$  being the experimental critical temperature. In tin  $(\omega_D/\omega_c)^3 = 254$  or  $T_c \approx 940$  K (Table II). Indeed we find  $T_c$

 TABLE IV. Properties calculated for superconducting elements when  $\omega_c$  is replaced by  $\omega_D$ .

	$\Delta(0)^a$	$2\Delta(0)/k_B T_c$	$T_c^b$	$T_c^c$
Zn	2830	5.67	590	190
Cd	600	5.13	140	40
Hg	6700	5.47	1440	2180
Al	3040	5.62	640	190
Ga	11550	5.78	2350	1230
In	1680	5.72	350	400
Tl	2120	5.80	430	1020
Sn	4810	5.74	980	940
Pb	5270	5.51	1120	1760
V	51980	4.86	12550	17110
Nb	21470	5.01	5020	7760
Ta	18200	5.29	4040	5230

<sup>a</sup>In  $10^{-4}$  eV.

<sup>b</sup>In K.

<sup>c</sup>From Eq. (59), in K.

=980 K for tin when we use  $\xi_D$  to replace  $\xi_c$  in Eq. (47). The gap function  $\Delta(\epsilon)$  then turns out to have many peaks with an erroneous  $2\Delta(0)/k_B T_c$  value of 5.74 (Fig. 5). Data for other metals are listed in Table IV.

### XIII. CONCLUSIONS

It has been shown in a field theoretic argument that inclusion of the repulsive Coulomb interaction between electrons does not result in weakening of the attractive electron-phonon interaction. What is affected is the dispersion relation of the electrons which has insignificant effect on  $T_c$ . Direct numerical calculation also demonstrates that  $T_c$  remains unchanged when the strength of Coulomb screening radius is varied. The BCS theory has been generalized to include consideration of the adiabatic parameter,  $\delta$ , which reflects essential information about the electron and phonon model employed. Also included in consideration is the phonon cutoff frequency  $\omega_c$  which is much lower than the Debye frequency, consistent with the view in Ref. 6 that superconductivity is frustrated once umklapp scattering occurs. This modest extension of BCS theory brings handsome reward in that the well-known ratio 3.5 is replaced by a range of more realistic ratios, varying from 3.51 for Ga to 4.76 for Hg. It is also rewarding to realize that there is room to raise  $T_c$  significantly if the frustration effect of umklapp scattering could somehow be eased or lifted.

### ACKNOWLEDGMENTS

The authors wish to thank Professor R. Atkinson for helpful suggestions.

### APPENDIX

We prove the following operator expansion formula:

$$e^{-S} H e^S = H + \sum_{n=1}^{\infty} \frac{1}{n!} C_n(H, S) \quad (\text{A1})$$

by analogy to the Taylor series, where

$$C_n(H, S) = [\underbrace{[\dots [H, S], S], \dots, S}]_n \quad (\text{A2})$$

is the  $n$ -fold commutation relation,  $[A, B] = AB - BA$ . When we use the definition  $\exp(\pm S) = \sum_n (\pm S)^n / n!$  to expand  $e^{-S} H e^S$  and collect all the terms where the total number of  $S$  is  $n$ , we find

$$e^{-S} H e^S = H + \sum_{n=1}^{\infty} \sum_{m=0}^n \frac{(-1)^m}{m!(n-m)!} S^m H S^{n-m}. \quad (\text{A3})$$

Equation (A1) follows if we can prove

$$\frac{1}{n!} C_n(H, S) = \sum_{m=0}^n \frac{(-1)^m}{m!(n-m)!} S^m H S^{n-m}. \quad (\text{A4})$$

Apparently Eq. (A4) is valid when  $n=1$ . If this is also the case for arbitrary  $n$  then

$$\begin{aligned} \frac{1}{(n+1)!} C_{n+1}(H, S) &= \frac{1}{n+1} \left[ \frac{1}{n!} C_n(H, S), S \right] \\ &= \frac{1}{n+1} \sum_{m=0}^n \frac{(-1)^m}{m!(n-m)!} (S^m H S^{n-m+1} - S^{m+1} H S^{n-m}) \\ &= \frac{1}{n+1} \sum_{m=0}^n \frac{(n+1-m)(-1)^m}{m!(n+1-m)!} S^m H S^{n+1-m} + \frac{1}{n+1} \sum_{m=0}^n \frac{(m+1)(-1)^{(m+1)}}{(m+1)!(n+1-m-1)!} S^{m+1} H S^{n+1-m-1} \\ &= \sum_{m=0}^n \frac{n+1-m}{n+1} \frac{(-1)^m}{m!(n+1-m)!} S^m H S^{n+1-m} + \sum_{m=1}^{n+1} \frac{m}{n+1} \frac{(-1)^m}{m!(n+1-m)!} S^m H S^{n+1-m} \\ &= \sum_{m=0}^{n+1} \frac{(-1)^m}{m!(n+1-m)!} S^m H S^{n+1-m}. \end{aligned} \quad (\text{A5})$$

The induction is complete.

\*Electronic address: xhz@qub.ac.uk

<sup>1</sup>J. Bardeen, L. N. Cooper, and J. R. Schrieffer, Phys. Rev. **108**, 1175 (1957).

<sup>2</sup>D. Pines, Phys. Rev. **109**, 280 (1957).

<sup>3</sup>J. B. Ketterson and S. N. Song, *Superconductivity* (Cambridge

University Press, Cambridge, 1999).

<sup>4</sup>M. Tinkham, *Superconductivity* (McGraw-Hill, New York, 1996).

<sup>5</sup>H. Fröhlich, Proc. R. Soc. London, Ser. A **215**, 291 (1952).

<sup>6</sup>X. H. Zheng and D. G. Walmsley, J. Phys.: Condens. Matter **16**, 8297 (2004).



- <sup>7</sup>J. M. Ziman, *Electrons and Phonons* (Oxford University Press, Oxford, 1960).
- <sup>8</sup>N. F. Mott and D. S. Jones, *The Theory of the Properties of Metals and Alloys* (Oxford University Press, Oxford, 1936).
- <sup>9</sup>M. B. Walker and M. F. Smith, Phys. Rev. B **61**, 11 285 (2000).
- <sup>10</sup>N. Fukukawa and T. M. Rice, J. Phys.: Condens. Matter **10**, L381 (1998).
- <sup>11</sup>P. L. Lee, Phys. Rev. Lett. **71**, 1887 (1993).
- <sup>12</sup>E. G. Maksimov, D. Yu. Savrasov, and S. Yu. Savrasov, Phys. Usp. **40**, 337 (1997).
- <sup>13</sup>J. P. Carbotte and R. C. Dynes, Phys. Lett. **25A**, 532 (1967).
- <sup>14</sup>J. P. Carbotte and R. C. Dynes, Phys. Rev. **172**, 476 (1968).
- <sup>15</sup>C. G. Kuper, Physica (Amsterdam) **24**, 304 (1958).
- <sup>16</sup>J. M. Rowell, P. W. Anderson, and D. E. Thomas, Phys. Rev. Lett. **10**, 334 (1963).
- <sup>17</sup>D. J. Scalapino, J. R. Schrieffer, and J. W. Wilkins, Phys. Rev. **148**, 263 (1966).
- <sup>18</sup>G. M. Eliashberg, Sov. Phys. JETP **11**, 696 (1960).